global genome demethylation and a loss of the ability to methylate newly integrated retroviral DNA (12). Dnmt3L is required specifically for the establishment of genomic imprints but is dispensable for their propagation, and *Dnmt3L* is the only gene known to be essential for the de novo methylation of single-copy DNA sequences. The results of this and prior studies (27) confirm that the methylation of single-copy sequences and repeated sequences are independently regulated. The sequence of Dnmt3L suggests that the protein is likely to function not directly as a DNA methyltransferase but as a regulator of methylation at imprinted loci, and identification and characterization of germ cell factors that interact with Dnmt3L should lead to a better understanding of the mechanisms that establish genomic imprints.

References and Notes

1. J. McGrath, D. Solter, *Cell* **37**, 179 (1984).
2. S. C. Barton, M. A. Surani, M. L. Norris, *Nature* **311**, 374 (1984).
3. A. Efstratiadis, *Curr. Opin. Genet. Dev.* **4**, 265 (1994).
4. Reviewed in S. M. Tilghman, *Cell* **96**, 185 (1999).
5. B. Tycko, *Probl. Cell Differ.* **25**, 133 (1999).
6. D. Humpherys et al., *Science* **293**, 95 (2001).
7. T. Kono, Y. Obata, T. Yoshimzu, T. Nakahara, J. Carroll, *Nature Genet.* **13**, 91 (1996).
8. T. L. Davis, G. J. Yang, J. R. McCarrey, M. S. Bartolomei, *Hum. Mol. Genet.* **9**, 2885 (2000).
9. T. Ueda et al., *Genes Cells* **5**, 649 (2000).
10. R. Stoger et al., *Cell* **73**, 61 (1993).
11. U. Aapola et al., *Genomics* **65**, 293 (2000).
12. M. Okano, S. Xie, E. Li, *Nature Genet.* **19**, 219 (1998).
13. S. Klimasauskas, S. Kumar, R. J. Roberts, X. Cheng, *Cell* **76**, 357 (1994).
14. C. L. Halbert, I. E. Alexander, G. M. Wolgamot, A. D. Miller, *J. Virol.* **69**, 1473 (1995).
15. A. J. Copp, *Trends Genet.* **11**, 87 (1995).
16. S. J. Clark, J. Harrison, C. L. Paul, M. Frommer, *Nucleic Acids Res.* **22**, 2990 (1994).
17. C. C. Glenn, K. A. Porter, M. T. Jong, R. D. Nicholls, D. J. Driscoll, *Hum. Mol. Genet.* **2**, 2001 (1993).
18. M. S. Bartolomei, A. L. Webber, M. E. Brunkow, S. M. Tilghman, *Genes Dev.* **7**, 1663 (1993).
19. A. C. Ferguson-Smith, H. Sasaki, B. M. Cattanach, M. A. Surani, *Nature* **362**, 751 (1993).
20. M. Bartolomei, personal communication.
21. P. E. Szabo, J. R. Mann, *Genes Dev.* **9**, 3097 (1995).
22. S. Horike et al., *Hum. Mol. Genet.* **9**, 2075 (2000).
23. N. J. Smilinich et al., *Proc. Natl. Acad. Sci. U.S.A.* **96**, 8064 (1999).
24. M. A. Cleary et al., *Nature Genet.* **29**, 78 (2001).
25. E. Li, T. H. Bestor, R. Jaenisch, *Cell* **69**, 915 (1992).
26. T. H. Bestor, *Hum. Mol. Genet.* **9**, 2395 (2000).
27. C. Y. Howell et al., *Cell* **104**, 829 (2001).
28. G.-L. Xu et al., *Nature* **402**, 187 (1999).
29. D. Bourc'his, T. H. Bestor, data not shown.
30. C. P. Walsh, J. R. Chaillet, T. H. Bestor, *Nature Genet.* **20**, 116 (1998).
31. GenBank accession codes and expressed polymorphisms are as follows, with the *M. musculus* allele preceding and the *M. m. castaneus* allele following nucleotide position: Snrpn: MMSMM, C915T; Kcnq1ot1: AF119385, T3976G; Zfp127: MMU19106, G1544AATGCCT; Ndn: MUSNECDIN, T117C; Peg3: AF038939, A3451G; Igf2: MMU71085, (CA)$_{18}$25435(CA)$_{21}$. Allele-specific expression of Igf2 was assessed by RT-PCR followed by digestion of the product with Nde I and Hae III and then separation of the fragments by agarose gel electrophoresis. H19 polymorphism was as described in (21). Sequences of PCR primers are available on request.
32. We are grateful to M. Mann and M. Bartolomei for providing unpublished data on expressed polymorphisms in imprinted genes and to J. R. Chaillet and M.

Requirement of Heterochromatin for Cohesion at Centromeres

Pascal Bernard,[1]*** Jean-François Maure,**[2]*** Janet F. Partridge,**[1]
Sylvie Genier,[2] **Jean-Paul Javerzat,**[2] **Robin C. Allshire**[1]†

Centromeres are heterochromatic in many organisms, but the mitotic function of this silent chromatin remains unknown. During cell division, newly replicated sister chromatids must cohere until anaphase when Scc1/Rad21–mediated cohesion is destroyed. In metazoans, chromosome arm cohesins dissociate during prophase, leaving centromeres as the only linkage before anaphase. It is not known what distinguishes centromere cohesion from arm cohesion. Fission yeast Swi6 (a Heterochromatin protein 1 counterpart) is a component of silent heterochromatin. Here we show that this heterochromatin is specifically required for cohesion between sister centromeres. Swi6 is required for association of Rad21-cohesin with centromeres but not along chromosome arms and, thus, acts to distinguish centromere from arm cohesion. Therefore, one function of centromeric heterochromatin is to attract cohesin, thereby ensuring sister centromere cohesion and proper chromosome segregation.

Before anaphase onset, each duplicated chromosome must be bilaterally attached to the mitotic spindle. This is achieved by sister centromeres and their associated kinetochores attaching to microtubules that emanate from opposite spindle poles. Accurate chromosome segregation requires that sister chromatids remain associated until all chromosomes have bilaterally attached to the spindle; only then can anaphase ensue. Sister chromatid cohesion is mediated by a conserved protein complex, known as cohesin (1). Anaphase is triggered by the cleavage of the Scc1/Rad21 subunit of cohesin allowing sister chromatid separation (2). In most organisms, cohesin is concentrated at centromeric regions (3–7). Metaphase chromosome spreads suggest that centromeres have a specialized role in holding sister chromatids together. Indeed, mammalian and fly cohesin is retained only at centromeric regions until anaphase (6, 7). What distinguishes cohesion at centromeres from cohesion along chromosome arms? The integrity of centromeric heterochromatin is known to be important for normal chromosome segregation, although its role has not been elucidated (8).

One possibility is that heterochromatin maintains cohesion between sister centromeres. Several observations suggest that heterochromatin may play a role in sister chromatid cohesion (9, 10). Here we demonstrate that the high concentration of cohesin and, thus, cohesion at centromeres is an intrinsic property of the underlying heterochromatin.

Schizosaccharomyces pombe (fission yeast) centromeres contain two distinct silenced chromatin domains composed of different proteins (11). Swi6 coats the outer repeat regions, whereas Mis6 and Cnp1 (the homolog of CENP-A) are restricted to the central domain (Fig. 1A). Mutations affecting these proteins alleviate transcriptional repression of a marker gene inserted only within their respective domains (11–13). Mutations or conditions that disrupt silencing over the outer repeats lead to a high incidence of lagging chromosomes on late anaphase spindles (14–16).

Recently, it has been shown that Rad21 strongly associates with the outer repeat regions (5, 17). To test for a link between outer repeat chromatin and cohesion, a strain was used in which Swi6 synthesis was driven by the repressible *nmt1* promoter (18). Growth in the presence of thiamine represses *swi6+* expression. Although Swi6 alone is not essential for cell viability, its withdrawal from *rad21-K1* cells (conditionally defective in cohesin function) (5) results in loss of viability (Fig. 1, B and C). Synthetic lethality often indicates functional

[1]MRC Human Genetics Unit, Western General Hospital, Crewe Road, Edinburgh EH4 2XU, UK. [2]Institut de Biochimie et Génétique Cellulaires, CNRS, Unité Mixte de Recherche 5095, 1 Rue Camille Saint Saëns, 33077 Bordeaux Cedex, France.

*These authors contributed equally to this work.
†To whom correspondence should be addressed. E-mail: robin.allshire@hgu.mrc.ac.uk

interactions. In support of this, *rad21-K1* cells display a high rate of lagging chromosomes at both permissive and restrictive temperatures (Fig. 1D), as previously observed in *swi6Δ* cells (*14*).

To further investigate the functional interac-

Fig. 1. The *rad21-K1* and *swi6Δ* mutations are synthetically lethal. (**A**) Symmetrical organization of fission yeast *cen1* (~35 kb). Swi6 coats the outer inverted repeats; Mis6 and Cnp1 are restricted to the central domain. Vertical lines in imr1 indicate tRNA genes. (**B**) Thiamine (Thi) was added to synthetic media (20 μM final concentration) to repress the *nmt1* promoter. Equal numbers of cells were plated onto media with or without thiamine. Wt, wild-type cells. (**C**) Swi6 and α-tubulin were detected by Western blotting with affinity-purified antibodies to Swi6 (*14*) and monoclonal TAT1 antibodies. Total protein extracts were prepared from cells grown in the presence (for 24 hours) or absence of thiamine at 25°C. (**D**) Asynchronous cultures were fixed at 25°C or after 4 hours (one doubling) at 36°C. Cells were stained with TAT1 (α-tubulin) and 4′,6′-diamidino-2-phenylindole (DAPI) (DNA) (*14*). One hundred late anaphase cells (spindle >5 μm) were examined for DAPI staining distant from the spindle poles (lagging chromosomes). Bar, 5 μm.

tion between Swi6 and Rad21, sister chromatid cohesion was examined in *swi6Δ* cells by fluorescent in situ hybridization (FISH) with the use of chromosome 1 cosmids as probes (*19*). Cells were arrested in metaphase by the *cut9-665* mutation (defective Anaphase Promoting Complex) (*20*). At the restrictive temperature (36°C), *cut9-665* cells arrest at metaphase with short spindles and unseparated sister chromatids, as revealed by the single FISH signals produced by the centromere proximal and arm probes (Fig. 2A). In contrast, *cut9-665 rad21-K1* cells displayed two separated FISH signals with both probes, demonstrating a complete lack of cohesion. In the absence of Swi6 (*swi6Δ*), sister centromeres clearly separate, forming two distinct signals distributed along the spindle axis in *cut9* arrested cells. However, the distal arm probe only produced one spot, indicating that cohesion along chromosome arms remained intact. To define more precisely the extent of the cohesion defect in *swi6Δ* cells, FISH was performed with cosmids positioned at increasing distances from *cen1* (Fig. 2B). Again, single signals were detected in *cut9-665 swi6Δ* cells for the most distal cosmid probes, whereas in *cut9-665 rad21-K1* cells both the centromere proximal and chromosome arm probes produced a signal that was usually separated into two spots. These data indicate that a Swi6 deficiency specifically disrupts cohesion at the centromere but not along the chromosome arms.

The high concentration of cohesin at centromeres may counteract spindle forces across sister centromeres due to bilateral spindle attachment. Therefore, we asked whether sister-centromeres in *swi6Δ cut9-665* cells still separate in the absence of microtubules. Figure 2C shows that when spindles are destroyed in these cells, sister centromeres are no longer resolved. Thus, remaining arm cohesion is sufficient to hold sister centromeres together when not subjected to opposing traction forces.

The above data indicate that Swi6 specifically influences cohesion at and nearby centromeres. One possibility is that Swi6 is required for association of cohesin with centromeres. The endogenous *rad21* open reading frame (ORF) was tagged with the 3xHA epitope, and association of Rad21-3xHA with centromeres was examined by chromatin immunoprecipitation
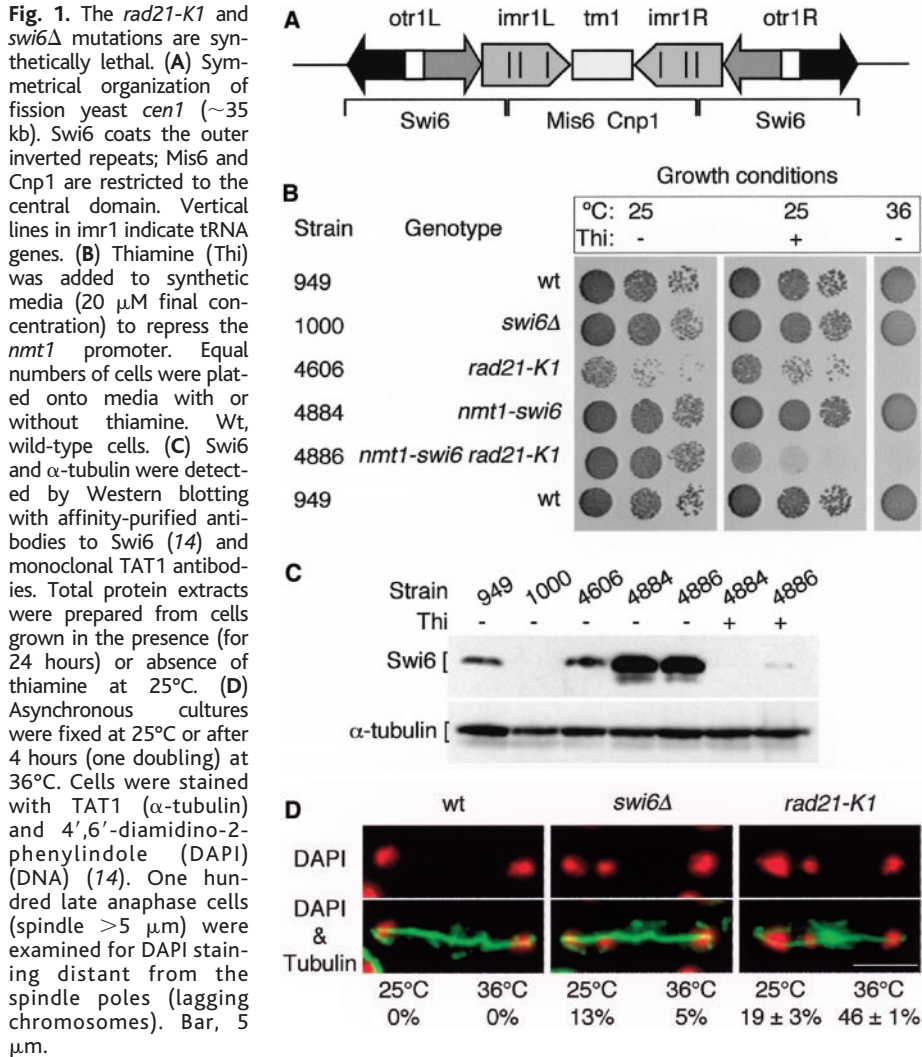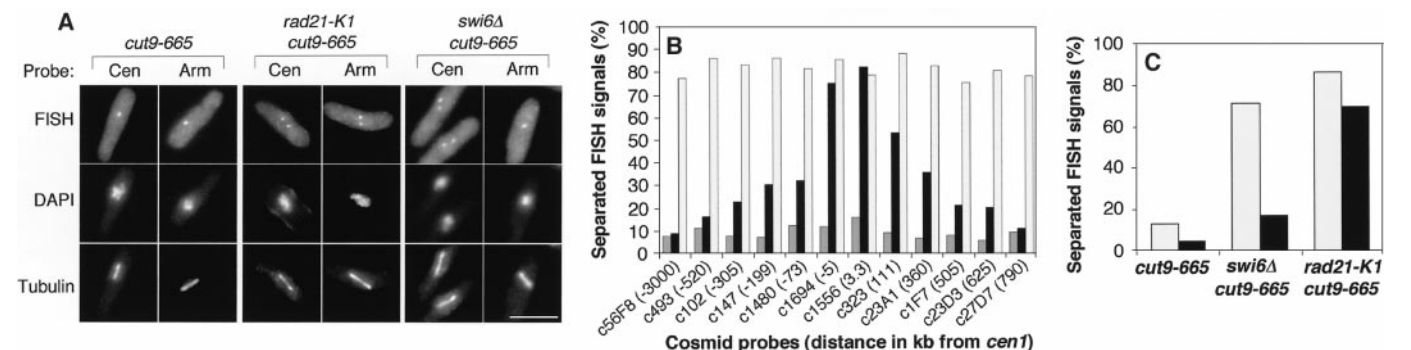

Fig. 2. Lack of Swi6 disrupts only sister centromere cohesion. Cells were shifted to 36°C for 4 hours (metaphase arrest), fixed, stained for tubulin, and hybridized with cosmid probes (*29*). More than 100 cells were examined for each sample. (**A**) Cosmids SPAC1694 and SPAC56F8 were used to monitor cohesion near *cen1* (Cen) and ~3000 kb away from *cen1* (left arm, Arm), respectively. Bar, 5 μm. (**B**) Co-

hesion integrity along chromosome 1. Black, *cut9-665 swi6Δ*; light gray, *cut9-665 rad21-K1*; dark gray, *cut9-665*. (**C**) *cut9-665* metaphase-arrested cells were treated with Benomyl (microtubule poison) at 200 μg/ml in dimethyl sulfoxide (DMSO) (black) or with DMSO alone (gray) before centromeric cohesion was monitored by FISH (cosmid SPAC1556).

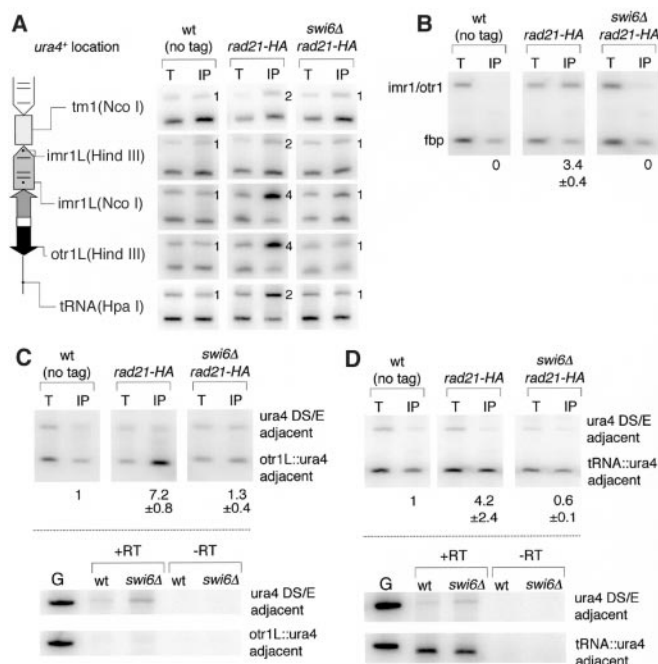(ChIP) (*11*) in wild-type and *swi6Δ* cells. This assay measures Rad21-3xHA association with *ura4+* inserted within the outer repeats or central domain of *cen1*. Untagged wild-type cells provide a convenient negative control. In wild-type cells, Rad21-3xHA associates mainly with the outer repeats and less with the central domain (Fig. 3A) (*5, 17*). However, in *swi6Δ* cells association of Rad21-3xHA with *ura4+* insertions in the outer repeats is lost. Similar results were obtained with *swi6Δ* cells arrested in early mitosis (*19*). Thus, Rad21 dissociation was not caused by cell cycle perturbation in *swi6Δ* cells. In *Saccharomyces cerevisiae*, cohesin is frequently associated with nontranscribed regions; transcription may block cohesin binding (*3, 4*). Because deletion of *swi6* allows expression of a normally silent *ura4+* residing in outer repeats (*12*), loss of Rad21 might be restricted to the transcribed marker. However, Rad21-3xHA association with native centromeric sequences is also dependent on Swi6 (Fig. 3, B and C, upper panel), and some centromeric sequences remain transcriptionally inert even in the absence of Swi6 (Fig. 3C, lower panel). In addition, Rad21 associates with DNA sequences near the centromere proximal tRNA, which are transcriptionally active in the presence or absence of Swi6 (Fig. 3D). Rad21 association with this transcriptionally active sequence is still dependent on the presence of Swi6. This clearly demonstrates that Swi6 is crucial for association of Rad21 across the centromere and provides a simple explanation for the lack of cohesion between sister centromeres in *swi6Δ* cells.

Examination of Rad21-3xHA association with chromosome arms required the identification of cohesion sites along chromosome 1. In *S. cerevisiae*, cohesin preferentially binds intergenic regions (*4*). Primer pairs were designed to assess enrichment of several intergenic regions within cosmids c8C9 (centromere proximal) and c56F8 (centromere distal) in anti-Rad21-3xHA immunoprecipitates (*19*). Polymerase chain reaction (PCR) conditions gave linear amplification of product from serial dilution of genomic DNA [see Web fig. 1 (*19*)]. This allowed enrichment of sequences in immunoprecipitates to be quantified relative to total cell extracts. Figure 4A shows two negative and seven positive arm sites. Rad21-3xHA is enriched at these positive sites, even in the absence of Swi6. Therefore, we conclude that Swi6 is required for the association of Rad21 at centromeres but not along chromosome arms, consistent with the observation that arm cohesion is maintained in the absence of Swi6 (Fig. 2A).

In *S. cerevisiae*, kinetochore function is required to recruit high concentrations of centromeric cohesin (*3*). It is possible that in fission yeast Swi6 heterochromatin only influences the recruitment of Rad21 in the context of a functional centromere. Alternatively, silent chromatin itself may suffice. Swi6 is not only associated with centromeres but contributes to heterochromatin at the mating type loci (*mat2-mat3*) and telomeres (*11, 12, 14*). Association of Rad21-3xHA with silent *ura4+* inserted adjacent to *mat3* or next to a telomere was examined (Fig. 4B). In both cases, Rad21-3xHA

Fig. 3. Swi6 attracts Rad21 to centromeric regions. Rad21-3xHA distribution across cen1 was determined by ChIP with antibodies to the HA epitope. T, total extract; IP, immunoprecipitated sample. (**A**) Competitive PCR assay for enrichment of ura4 within *cen1* (upper band) over the *ura4-DS/E* minigene (lower band). Enrichment was calculated as follows: the *ura4:ura4-DS/E* ratio of the IP was divided by the *ura4* versus *ura4-DS/E* ratio of the total extract. Values were normalized to their respective untagged controls. (**B**) Multiplex PCR assay for the imr1/otr1 junction PCR products (imr1/otr1) relative to the *fbp1* control (fbp). (**C** and **D**) Upper panels: Semi-competitive PCR (*11*) shows Rad21-3xHA association with native sequences adjacent to otr1L(Hind III)::*ura4+* and tRNA(Hpa I)::*ura4+*. Primer 1 is anchored 800 bases upstream of the first codon of the ura4 (ATG) (also detects *ura4-DS/E*). Primer 2 corresponds to sequence neighboring otr1L(Hind III) or tRNA(Hpa I). Primer 3, adjacent to ura4-DS/E, yields the larger product. Lower panels: The same primers were used to amplify cDNA generated by RT-PCR from total RNA primed within *ura4*. G: genomic DNA.

Fig. 4. Rad21 association along chromosomes arms is Swi6-independent. (**A**) For each cosmid, ORFs (arrowheads) and intergenic regions (bars) are represented (not to scale), and coordinates of PCR primers are indicated. Rad21 enrichment at cen1 otr1L(Hind III) is shown for comparison. For numerical values, see Web table 1 (*19*). (**B**) Rad21-3xHA distribution at the mating-type locus and left telomere of chromosome 1 was determined by ChIP with antibodies to the HA epitope. Competitive PCR assay for enrichment of ura4 (upper band) inserted adjacent to *mat3* or next to the telomere, relative to the *ura4-DS/E* minigene (lower band). (**C**) Upper panel: Semi-competitive PCR (*11*) to assess Rad21 association with native telomeric associated sequences (TAS) adjacent to *ura4*. Primers 1 and 3 are as in Fig. 3. Primer 2 corresponds to TAS neighboring *ura4*. Lower panel: The same primers were used to amplify cDNA generated by RT-PCR from total RNA primed within *ura4*. G: genomic DNA.
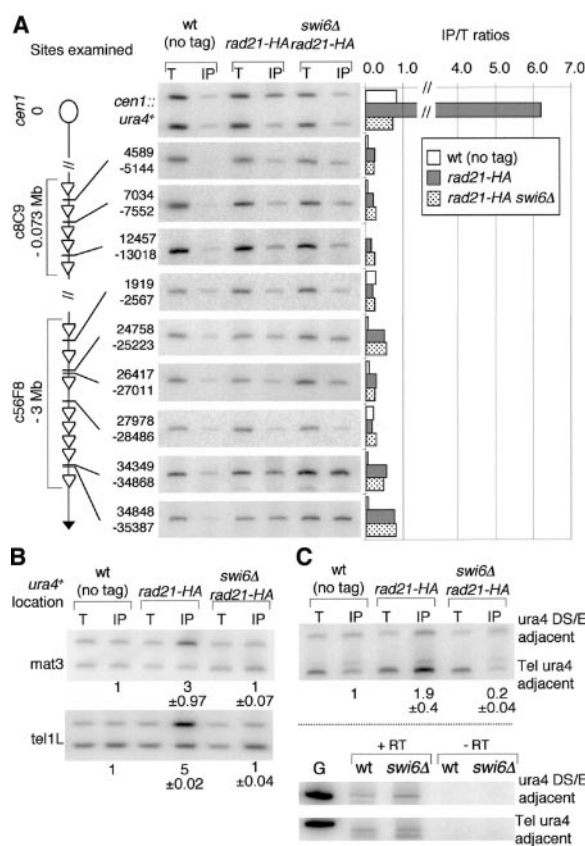
coated these silent *ura4*⁺ genes and association was abolished in *swi6*Δ cells. This dissociation of Rad21 cannot be attributed to transcriptional interference because Rad21-3xHA also coats the telomere adjacent sequence, which is transcribed in *swi6*⁺ and *swi6*Δ cells (Fig. 4C). Therefore, these data indicate that silent Swi6 chromatin alone forms domains with a high affinity for Rad21-cohesin and that the high concentration of cohesin over centromeric regions occurs outside of the context of a functional kinetochore.

Clr4 [equivalent to mammalian and fly Su-(var)39] methylates histone H3 on lysine-9 (*21*, *22*), Swi6 association with centromeres requires this activity, and the chromo-domain of Swi6 binds specifically to histone H3 NH₂ termini only when methylated on lysine-9 (*23*). The assembly of this silent Swi6 chromatin is required to attract cohesin to centromeres, because centromere association of Rad21 and another cohesin component, Psc3 (*5*), were dependent on Swi6 (*19*). Many mutants known to alter this heterochromatin coating the outer repeats of fission yeast centromeres lose chromosomes and have a high incidence of lagging chromosomes on late anaphase spindles (*12*, *14*, *16*). Figure 1D shows that the major segregation defect observed when Rad21-cohesin function is perturbed is also anaphase-lagging chromosomes. Lagging chromosomes are mostly single separated chromatids (*16*). A similar defect is observed in trichostatin A–treated cells, where mouse Heterochromatin protein 1 (HP1) or *S. pombe* Swi6 are also mislocalized (*15*, *24*). In rat kangaroo PtK1 cells, most lagging chromosomes are single chromatids resulting from the attachment of an individual kinetochore on the laggard to microtubules from both poles (*25*) (merotelic attachment). In metazoans, cohesin persists only between the heterochromatic domains of sister centromeres at metaphase (*6*, *7*). Thus, as in fission yeast, lagging chromosomes may result from defective centromeric cohesion due to HP1 dispersal. Intriguingly, lagging chromosomes have not been reported in any mutant defective in centromere or cohesin function in budding yeast. Indeed, the major mitotic defect observed in *S. cerevisiae* cells lacking cohesin is nondisjunction (*26*). *S. cerevisiae* kinetochores have been shown to bind only one microtubule (*27*), and centromeric heterochromatin has not been described. In contrast, *S. pombe* centromeres are packaged in heterochromatin and bind two to four microtubules (*28*) and, thus, have the capacity for merotelic attachment.

We propose that one function of silent Swi6 chromatin at fission yeast centromeres is to attract a high concentration of cohesin so that sister kinetochores face away from each other. The architecture formed by this silent chromatin in cooperation with cohesin might, therefore, aid the arrangement of multiple microtubule attachment sites at each sister kinetochore so that all sites at one kinetochore capture microtubules from the same pole. Assuming that this role for centromeric heterochromatin is conserved, we expect that deficiencies in heterochromatin formation will contribute to aberrant mitotic and meiotic chromosome segregation in humans, driving tumor formation and the production of aneuploid offspring.

References and Notes

1. K. J. Dej, T. L. Orr-Weaver, *Trends Cell Biol.* **10**, 392 (2000).
2. F. Uhlmann, F. Lottspeich, K. Nasmyth, *Nature* **400**, 37 (1999).
3. T. Tanaka, M. P. Cosma, K. Wirth, K. Nasmyth, *Cell* **98**, 847 (1999).
4. S. Laloraya, V. Guacci, D. Koshland, *J. Cell Biol.* **151**, 1047 (2000).
5. T. Tomonaga *et al.*, *Genes Dev.* **14**, 2757 (2000).
6. I. C. Waizenegger, S. Hauf, A. Meinke, J. M. Peters, *Cell* **103**, 399 (2000).
7. W. D. Warren *et al.*, *Curr. Biol.* **10**, 1463 (2000).
8. G. H. Karpen, R. C. Allshire, *Trends Genet.* **13**, 489 (1997).
9. D. R. Wines, S. Henikoff, *Genetics* **131**, 683 (1992).
10. G. H. Karpen, M. H. Le, H. Le, *Science* **273**, 118 (1996).
11. J. F. Partridge, B. Borgstrom, R. C. Allshire, *Genes Dev.* **14**, 783 (2000).
12. R. C. Allshire, E. R. Nimmo, K. Ekwall, J. P. Javerzat, G. Cranston, *Genes Dev.* **9**, 218 (1995).
13. A. L. Pidoux, R. C. Allshire, unpublished data.
14. K. Ekwall *et al.*, *Science* **269**, 1429 (1995).
15. K. Ekwall, T. Olsson, B. M. Turner, G. Cranston, R. C. Allshire, *Cell* **91**, 1021 (1997).
16. A. L. Pidoux, S. Uzawa, P. E. Perry, W. Z. Cande, R. C. Allshire, *J. Cell Sci.* **113**, 4177 (2000).
17. Y. Watanabe, S. Yokobayashi, M. Yamamoto, P. Nurse, *Nature* **409**, 359 (2001).
18. P. Bernard, K. Hardwick, J. P. Javerzat, *J. Cell Biol.* **143**, 1775 (1998).
19. Supplemental material is available at *Science* Online at www.sciencemag.org/cgi/content/full/1064027/DC1.
20. H. Yamada, K. Kumada, M. Yanagida, *J. Cell Sci.* **110** (15), 1793 (1997).
21. J. Nakayama *et al.*, *Science* **292**, 110 (2001).
22. S. Rea *et al.*, *Nature* **406**, 593 (2000).
23. A. J. Bannister *et al.*, *Nature* **410**, 120 (2001).
24. A. Taddei, C. Maison, D. Roche, G. Almouzni, *Nature Cell Biol.* **3**, 114 (2001).
25. D. Cimini *et al.*, *J. Cell Biol.* **153**, 517 (2001).
26. T. Tanaka, J. Fuchs, J. Loidl, K. Nasmyth, *Nature Cell Biol.* **2**, 492 (2000).
27. E. T. O'Toole, M. Winey, J. R. McIntosh, *Mol. Biol. Cell* **10**, 2017 (1999).
28. R. Ding, K. L. McDonald, J. R. McIntosh, *J. Cell Biol.* **120**, 141 (1993).
29. Cosmids SPA c56F8 {37 kb}, c493 [37 kb], c102 [36 kb], c147 [37.7 kb], c1480 [36.8 kb], c1694 [44 kb] (including c8C9), c1556 [36.6 kb], c323 [39.3 kb], c23A1 {36 kb}, c1F7 {34 kb}, c23D3 {42 kb}, and c27D7 {36 kb} were used as FISH probes. These were identified at www.sanger.ac.uk/Projects/S_pombe/ and obtained from the Sanger Centre, UK. Square brackets indicate physical size, whereas curly brackets indicate the size of the sequenced portion of the cosmid. Cosmids were prepared and utilized for FISH, as previously described (*14*).
30. We thank Allshire lab members for helpful input, M. Yanagida for *cut9-665*, H. Ikeda for *rad21-K1*, and K. Gull for TAT1. Allshire lab centromere research is supported by MRC core funding. P.B. is supported by a Wellcome Trust Travelling Research Fellowship. Research in the Javerzat lab is supported by the Centre National de la Recherche Scientifique and l'Association pour la Recherche sur le Cancer and J.-F.M., by a fellowship from the Ministère de la Recherche et de l'Enseignement Supérieur.

Stem Cell Self-Renewal Specified by JAK-STAT Activation in Response to a Support Cell Cue

Amy A. Kiger,[1]*† D. Leanne Jones,[1]* Cordula Schulz,[1] Madolyn B. Rogers,[1] Margaret T. Fuller[1,2]‡

Stem cells generate many differentiated, short-lived cell types, such as blood, skin, and sperm, throughout adult life. Stem cells maintain a long-term capacity to divide, producing daughter cells that either self-renew or initiate differentiation. Although the surrounding microenvironment or "niche" influences stem cell fate decisions, few signals that emanate from the niche to specify stem cell self-renewal have been identified. Here we demonstrate that the apical hub cells in the *Drosophila* testis act as a cellular niche that supports stem cell self-renewal. Hub cells express the ligand Unpaired (Upd), which activates the Janus kinase–signal transducer and activator of transcription (JAK-STAT) pathway in adjacent germ cells to specify self-renewal and continual maintenance of the germ line stem cell population.

Stem cell self-renewal must be regulated to avoid either stem cell loss or hyperproliferation. In some systems stem cell numbers are limited by asymmetric cell division, where one daughter cell retains stem cell identity, while the other initiates differentiation. However, stem cells can also divide symmetrically to expand stem cell numbers after wound-